# Analyst

Accepted Manuscript


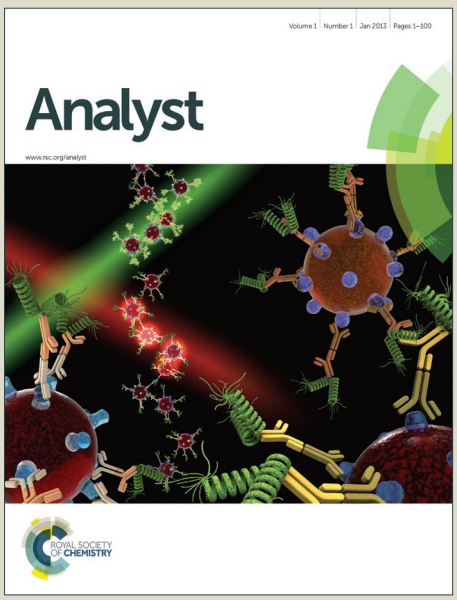





ROYAL SOCIETY OF CHEMISTRY

www.rsc.org/analyst

# Nanomaterials-based approaches for the detection and speciation of mercury

Xiaohan Xu [1,2], Yu-Feng Li[1]*, Jiating Zhao[1], Yunyun Li [1,2], Jing Lin [1], Bai Li[1], Yuxi Gao[1], Chunying Chen[3]

[1]CAS Key Laboratory for Biomedical Effects of Nanomaterials and Nanosafety, and State Environmental Protection Engineering Center for Mercury Pollution Prevention and Control, Institute of High Energy Physics, Chinese Academy of Sciences, Beijing 100049, China

[2]University of Chinese Academy of Sciences, Beijing 100049,China.

[3] National Center for Nanoscience and Technology, Beijing 100190, China

*Corresponding auhtor: Email: liyf@ihep.ac.cn,Tel: +86-10-88233908, Fax: +86-10-88235294

**TOC entry**

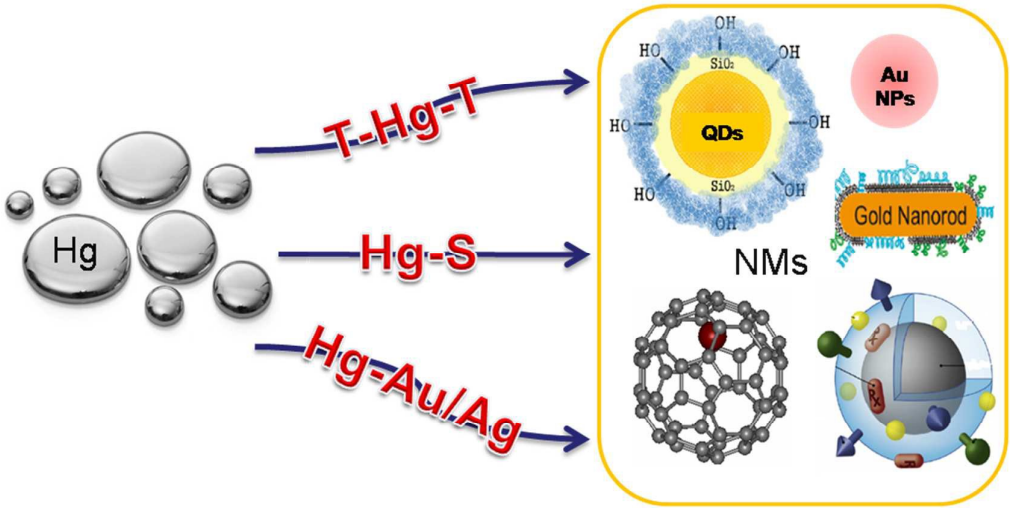


Detection and speciation of Hg through the T-Hg-T coordination, Hg-S and/or Hg-Au/Ag interactions based colorimetric or fluorescent changes

**Abstract**

Mercury is toxic with widespread contamination. Highly sensitive and selective approaches for mercury analysis are desired. Although conventional techniques are accurate and sensitive in the determination of mercury, these procedures are time-consuming, labor-intensive and dependent heavily on expensive instrumentation. In recent years, nanomaterials-based approaches have been proved to be effective alternatives in the detection and speciation of mercury. In this review, the development of different nanomaterials-based approaches was summarized, as well as their utilization for the detection of mercury in environmental and biological samples, such as gold nanomaterials, carbon nanomaterials and quantum dots and so on. Moreover, the speciation of mercury using nanomaterials was also reviewed.

## 1. Introduction

Mercury (Hg) is a widespread global contaminant due to its distinct toxicity and accumulative properties that are harmful to the environment and human beings, as seen in unfortunate incidents as Minamata disease and mercury poisoning in Iraq.[1] It can cause neurological and developmental impairments such as decrements in attention, language, verbal memory, visuospatial function and IQ impairment even at low level, especially for the *in utero* and early postnatal exposure.[2-6]

Routine monitoring of mercury is important for environmental and human health protection. Commercial instruments, such as atomic absorption/emission spectroscopy (AAS/AES),[7, 8] atomic fluorescent spectroscopy (AFS),[9] electrochemistry,[10] chromatography,[11, 12] inductively coupled plasma-atomic emission spectrometry (ICP-OES),[13] inductively coupled plasma mass spectrometry (ICP-MS)[14, 15]have been extensively used in the monitoring of Hg in different matrixes. Despite the high accuracy and sensitivity of these techniques in the detection and speciation of mercury in various sample matrixes, they are time-consuming, labor-intensive and dependent heavily on expensive instrumentation. Furthermore, most of them are not suitable for the on-site monitoring. In recent years, various strategies based on small organic chromophores or fluorophores,[16-19] conjugated polymers,[20] oligonucleotides,[21, 22]DNAzymes,[23] or G-quadruplex[24] etc. have been developed aiming for the on-site and low-cost detection of Hg.Although these probes provided alternative means to measure Hg, they had many drawbacks such as lack of water solubility, low-selectivity toward other metal ions, and relative high detection limit comparing to routine methods. Furthermore, the application of these methods to real samples especially complex samples was rarely reported.

Nanomaterials are materials having sizes in the range 1-100nm, and they have uniquely physical and chemical properties distinctive from their bulk counterparts, which make them promising candidates for signal generation and transduction in detection of various analytes.[25, 26] The large surface-to-volume ratio of nanoparticles can increase the sensitivity and make miniaturization of the devices possible. Besides,

nanoparticles can be modified with functional groups which are specific for Hg detection. Therefore, nanomaterials have shown great potential for high sensitivity, selectivity and rapid detection and speciation of Hg. In the present review, nanomaterials used in the detection and speciation of Hg were summarized and their underlying mechanism was also discussed.

## 2. Detection of mercury

### 2.1 Gold nanomaterials

Gold nanomaterials are the most intensively studied nanomaterials that are used for the detection of mercury and other metal ions because of their strong surface plasmon resonance absorptions in the visible region, high stability and biocompatibility and the simple preparation.[27] Besides, mercury and gold can form amalgams and this has also been used for the detection of Hg.[28] Gold nanoparticles (Au NPs), gold nanorods (Au NRs) and gold nanoclusters (Au NCs) have been applied for the detection of Hg.

#### 2.1.1 Gold nanoparticles

Au NPs were developed for the determination of mercury due to their extremely high coefficients, strongly distance-dependent surface plasmon resonance absorption and excellent quenching fluorescence properties.[29] Au NPs could be used as colorimetric sensors in the on-site monitoring of Hg through the direct observation by naked eyes based on the color change of the solution under test.[30-33] Besides, Au NPs were widely applied as fluorescent sensors for mercury detection, which offered simple and rapid detection of $Hg^{2+}$ in environmental and biological samples.[34-36]

##### *2.1.1.1 Au NPs functionalized with DNA*

The surface plasmon resonance of Au NPs is size-dependent while mercuric ions have high affinity to thymine (T) bases to form T-$Hg^{2+}$-T coordination.[37] Therefore, the Au NPs functionalized with T-T mismatched DNA strands can be used to detect

Hg.[11, 38, 39] There are two types of DNA-Au NPs for mercury detection, which are "non-crosslink aggregation" and "inter-particles crosslink aggregation".

In non-crosslink aggregation, $Hg^{2+}$ coordinated with the short single-stranded DNA (ssDNA) or double-stranded DNA (dsDNA) from the surface of Au NPs, inducing the aggregation of Au NPs and the colorimetric changes.[40-42] Li et al.[40] demonstrated that Au NPs were stable in the presence of unmodified ssDNA with appropriate salt concentration in solution, but aggregated in the presence of $Hg^{2+}$ owing to the formation of $Hg^{2+}$ mediated hairpin structure of DNA in which $Hg^{2+}$ linked T residues of the nucleotides that were spatially separated by T-$Hg^{2+}$-T coordination. The addition of $Hg^{2+}$ caused the aggregation of NPs and the intensification of red-shifted band, which demonstrated that the visual rapid detection of $Hg^{2+}$ was possible. The determination limit of this method corresponded to 10 nM. Compared with traditional methods, this approach could achieve similar low detection limit and was much simpler and inexpensive in terms of instrumentation. Wu et al. [43]detected $Hg^{2+}$ on the basis of mercury-specific deoxyribonuclein acid functionalized Au NPs. With the addition of $Hg^{2+}$, the folded mercury-specific DNA strand was formed through T-$Hg^{2+}$-T coordination, which prevented the aggregation of Au NPs against high salt solution with the detection limit of 60 nM for $Hg^{2+}$ that was much lower than 2.4 μM, the toxicity level of $Hg^{2+}$ in edible fish samples defined by United States Environmental Protection Agency (U.S. EPA).Besides, this method guaranteed that $Hg^{2+}$ got the highest signal among all the other metal ions and made it possible that the inhibition degree of color change could be directly displayed by the amount of $Hg^{2+}$ in analytes, which made the system an ideal sensor to the detection of $Hg^{2+}$. In terms of application of this assay, the probe was applied to detect the determination of $Hg^{2+}$ in fish samples and the results was compared with that from Cold vapor atom adsorption spectroscopy (CVAAS). The comparison showed that the results were in keeping with the expected and found values. Another type of rapid non-crosslink aggregation based on double-stranded DNA-carrying gold nanoparticles (dsDNA-Au NPs) was also studied.[44] The method was based on the colloidal stability of dsDNA-Au NPs which depended on T-T mismatch embedded in the dsDNA that

modified on the surface of Au NPs. In the presence of $Hg^{2+}$, T-$Hg^{2+}$-T complex was formed which induced the color of the solutions to change from red to colorless. This method could achieve high selectivity without any masking reagents and temperature control, which were suitable for on-site environmental monitoring of various media polluted by toxic metal ions such as ponds, lakes, rivers and so on. Besides, the remarkable superiority of this approach over previous ones was that the detection of $Hg^{2+}$ with naked eyes could be finished within 1min by using minimized analytical procedures, which was much faster and easier to manipulate and simpler than traditional methods that were time-consuming and dependent on expensive instrumentation and intensive labor-force.

For the inter-particle crosslink aggregation, Lee et al. [45]designed two types of Au NPs functionalized with different thiolated-DNA sequences, which were complementary except for a single T-T mismatch (**Error! Not a valid bookmark self-reference.**). When two complementary DNA-Au NPs were combined, DNA-linked aggregation would occur which could dissociate reversibly with the color changing from purple to red at lower melting temperature. In presence of $Hg^{2+}$, it would interact with DNA-Au NPs via T-$Hg^{2+}$-T, which could stabilize the duplex DNA and increased the melting temperature of the DNA-Au NPs as compared with the situation without $Hg^{2+}$. The specific temperature at which aggregates melted with the significant color change from purple to red was directly related to the $Hg^{2+}$ content in analytes, which improved the selectivity and sensitivity of this method and made it distinguished from conventional analytical methods. The detection limit for $Hg^{2+}$ was 100nM at 47℃. Xue et al. [37] proposed a similar but more simple and economical strategy at room temperature to achieve the one-step detection for $Hg^{2+}$(Figure 9). They prepared two types of DNA functionalized Au NPs, which were not complementary and contained different numbers of thymine bases, and an appropriate oligonucleotide linker as three probes for $Hg^{2+}$ detection. In the absence of $Hg^{2+}$, these probes had lower melting temperature than that of DNA duplexes. Upon addition of $Hg^{2+}$, the melting temperature increased, induced the complexation of DNA-Au NPs aggregation and led to the color response from red to purple. The melting temperature

was in direct proportion to the concentration of $Hg^{2+}$. The detection limit for $Hg^{2+}$ was 3 μM by using 14nm Au NPs in this approach.

Liu et al. [42] designed an assay by fluorescence responses for sensitive and selective detection of $Hg^{2+}$ ions using both DNA-Au NPs and OliGreen. In this assay, $Hg^{2+}$ interacted with thymine, resulting in the conformation changes of the DNA on the surface of Au NPs from liner to hairpin structure, and a part of DNA molecules released from the surface of Au NPs. OliGreen molecules interacted with free DNA species, causing the fluorescence enhancement at 525nm, which was much stronger than free OliGreen or OliGreen interacted with DNA on surface of Au NPs. The sensitivity of the method was dependent on the density of DNA on the surface of Au NPs for that Au NPs were efficient fluorescence quenchers. The detection limit for $Hg^{2+}$ was 25nM. Researchers used this method to analyze a water sample from a pond and the results were in keeping with that from the conventional ICP-MS. This method had high selectivity and was applied for detection of $Hg^{2+}$ in the pond water samples, with recoveries among 96%-120% that displayed low matrix interference.

#### *2.1.1.2Au NPs functionalized with sulfur groups*

It is known that mercury has high affinity to thiol, therefore sulfur is introduced to detect$Hg^{2+}$ in Au NPs. Liu et al. [31]demonstrated a colorimetric detection of $Hg^{2+}$ (Figure 10).In the approach, (11-mercapto-undecyl) - trimethyl-ammonium (MTA) was capped on Au NPs through Au-S interactions and exhibited red color, which was only well-dispersed in acidic aqueous. In the presence of $Hg^{2+}$, it broke the Au-S bonds and caused the dissociation of MTA from Au NPs surface due to the high affinity to thiols of $Hg^{2+}$. So the aggregation of Au NPs happened and the color of solution turned from red to blue, which was demonstrated by the result of UV/Vis spectra. The detection limit for$Hg^{2+}$ was 30nM, with a detection range from $3\times10^{-8}$-1 $\times10^{-2}$M. It was found that organic mercury did not induce the aggregation of gold nanoparticles and only $Hg^{2+}$ caused color change of the solution in the existence of other environmentally relevant metal ions. The detection could be finished without any masking agents at room temperature. Compared with previous $Hg^{2+}$ detection

methods, this approach was much simpler for detecting $Hg^{2+}$ with better selectivity and sensitivity and solved the urgent need of advanced instruments in the detection of $Hg^{2+}$ and achieved the rapid detection that allowed naked-eye readout in resource-poor settings.

Biothiols were also used for the detection of mercuric ions. Du et al. [46]detected mercury through the interactions of biothiols with $Hg^{2+}$ (Figure 11). A linear oligopeptide (Lys-Cys-Gly-Trp-Gly-Cys) which consisted of natural thiol groups at both ends was designed as probes for $Hg^{2+}$. In this approach, the 13nm Au NPs showed a surface plasmon resonance band at 520nm with a red color. The color of Au NPs changed from red to blue when the oligopeptide was added into the solution and caused the aggregation of Au NPs to big clusters. In the presence of $Hg^{2+}$, the oligopeptide combined with $Hg^{2+}$first, thus lost the capability of inducing the aggregation of Au NPs. In this method, $Hg^{2+}$played a core role in preventing the aggregation of Au NPs caused by oligopeptides, which avoided false positives by spontaneous particle aggregation. This was different from other colorimetric based strategies. Furthermore, the strategy could be flexible for different concentration range (10nM to more than 100μM) of $Hg^{2+}$ detecting by adjusting the concentration of Au NPs or the oligopeptide, which also improved the sensitivity. When 0.54nM Au NPs and 0.1μM oligopeptide were employed in the system, the detection limit was 10 nM. The novelty of this assay was that the system could be obtained easily by one simple step of mixing the Au NPs with the oligopeptide and concentration of the oligopeptide could be adjusted to get better colorimetric performance, which could not be achieved by conventional methods such as AFS, ICP-OES, ICP-MS and some early colorimetric systems. The advantages of this assay allowed it to be promising in the on-site detection of $Hg^{2+}$ in complex media such as river water, industrial water and so on.

#### *2.1.1.3 Au NPs functionalized with fluorescent group*

The “turn on” and “turn off” of the fluorescence by $Hg^{2+}$ was also proposed using Au NPs. One classic “turn on” fluorescence sensor for $Hg^{2+}$ detection relied on

Rhodamine B (RB) capped-Au NPs (RB-Au NPs). RB exhibited high fluorescence in the bulk solution, but the fluorescence quenched when RB was absorbed on the surface of Au NPs. In the presence of $Hg^{2+}$, $Hg^{2+}$ bound with Au NPs and released RB from the surface of Au NPs. So the fluorescence of RB recovered. Zheng et al. [47] improved the sensitivity of the "turn on" method by modifying RB-Au NPs with thioglycolic acid (TGA). This approach displayed high selectivity for $Hg^{2+}$ with respect to other metal ions and low detection limit of $Hg^{2+}$ ($4\times10^{-10}$M). Hence, it has been utilized in the $Hg^{2+}$ detection of four water samples. All samples were got from local tap water, pond water and Yangtze River and filtered through filter paper before detection. The results were consistent with that obtained by AAS and the recoveries of $Hg^{2+}$ were among 98%-103%. In addition, TGA-modified Au NPs and Rhodanmine6G (R6G) were utilized on "turn on" of fluorescence for detecting of $Hg^{2+}$.[48] In this approach, the fluorescence of R6G was quenched by Au NPs when R6G was absorbed on the surface of Au NPs modified with TGA. After the addition of $Hg^{2+}$, the fluorescence of R6G was recovered and the color of solution changed from red to purple. This method provided a $Hg^{2+}$ detection limit of $6.0\times10^{-11}$M and obtained a satisfied recovery in the range of 96-102% when determining $Hg^{2+}$in water samples obtained from local tap and pond water.

Determination of $Hg^{2+}$ through the "turn off" of fluorescence was also reported. Huang et al. [49]designed a sensitive and selective fluorescence sensor for the detection of $Hg^{2+}$on the basis of aggregation-induced quenching of the fluorescence of the alkanethiol-Au NPs by $Hg^{2+}$. The alkanethiol-Au NPs, such as 11-mercaptoundecanoic acid-protected Au NPs (11-MUA-Au NPs),exhibited high fluorescence at 520nm with a quantum yield of 3.1%. In the presence of $Hg^{2+}$, aggregation-induced fluorescence quenching of 11-MUA-Au NPs happened. The fluorescence of 11-MUA-Au NPs decreased upon the increase of the concentration of $Hg^{2+}$, and the detection limit for $Hg^{2+}$ was as low as 5nM. With the PDCA as masking reagent, the selective for $Hg^{2+}$was at least 10-fold against $Pb^{2+}$ and $Cu^{2+}$, and 400 times for other metal ions. Researchers investigated the practicability of this assay during the $Hg^{2+}$ detection of a water sample obtained from a local pond and the result

showed that the $Hg^{2+}$ content in the pond sample was 3.49 ppb, which was in keeping with the 3.20 ppb detected by using ICP-MS. This method overcame many drawbacks brought by conventional analytical methods and achieved equally accurate results, which illustrated the superiority of novel analytical approach.

***2.1.1.4 Au NPs functionalized with nitrogen groups***

Except for the aforementioned detection systems, researchers have used Au NPs functionalized with some molecules rich of nitrogen to achieve the fast, simple and portable detection of mercury ion. Du et al.[50] built a melamine-Au NP system as a good $Hg^{2+}$ probe based on the coordination affinity between Melamine, a commercial heteocyclic-ring molecule containing multiple nitrogen and $Hg^{2+}$.It has been reported that melamine can lead to the aggregation of Au NPs in water based media by electrostatic effect. However, the addition of $Hg^{2+}$could prevent the aggregation of Au NPs caused by melamine for that the N atoms of melamine preferentially bond to $Hg^{2+}$and thus melamine lost the ability of aggregating Au NPs. This system exhibited a good linear relationship under the optimized conditions and the limit of detection (LOD)was 50nM, which illustrated that this system achieved excellent selectivity and sensitivity for $Hg^{2+}$ detection.

In order to be consistent with the goals of green chemistry and low consumption, Du et al.[51] chose to utilize a kind of natural product, urine, which owned similar binding sites to melamine to optimize the $Hg^{2+}$ detection system by simply mixing Au NPs solution and urine at an appropriate ratio based on coordination chemistry. In this assay, the 13nm Au NPs dispersed in aqueous solution with a red color SPR band at 520nm. There was little color change when urine was added to the solution and the components rich of nitrogen were adsorbed on the surface of the Au NPs. The addition of $Hg^{2+}$ however, caused an instant red-to-blue color change for that the $Hg^{2+}$ led to the crosslinking-induced aggregation of Au NPs based on coordination chemistry. This system showed great selectivity to $Hg^{2+}$ and good sensitivity which could be proved by the application in the detection of $Hg^{2+}$ in industrial wastewater. Besides, this work could be achieved by simply using urine and no complex ligand synthesis was needed, which exhibited that its simplicity, portability and

inexpensiveness made it very useful in remote and less industrialized areas. On the basis of this work, Du et al.[52] demonstrated the ability of uric acid and creatinine to bind $Hg^{2+}$on the surface of Au NPs synergistically and further successfully developed a uric acid and $Hg^{2+}$ modified AuNPs system to achieve the selective and effective detection of creatinine in complex matrix. This system achieved excellent sensitivity and selectivity of creatinine detection and showed its advantages such as simplicity, inexpensiveness and portability over other traditional detection methods, which could be helpful in the achievement of self-serviced clinical-sensing and monitoring of creatinine at home.

### 2.1.2 Gold nanorods and gold nanoclusters

Due to their uniquely optical and physiochemical properties such as simple surface modifications, anisotropic shape and so on, gold nanorods (Au NRs) have been widely applied in biomedicine[53-55] and chemical sensors.[56-58] Au NRs have two directional electron oscillations and exhibit two tunable surface plasmon resonance bands (SPR). The longitudinal and transversal plasmon bands correspond to the long and short axis of the Au NRs. The maximum absorption wavelength presents a linear correlation with the aspect ratio. For example, the band of longitudinal was red shifted when the aspect ratio increased.[59, 60]

Rex et al. [60] proposed a sensitive and selective method to determine $Hg^{2+}$ upon the absorption wavelength change of Au NRs based on affinity between gold and mercury. The procedure was simply to mix Au NRs with the sample present in sodium borohydride ($NaBH_4$), and no sample preparation was required, which displayed the simplicity of the design. In this method, Au NRs with the aspect ratio of 1.6 were used, and the longitudinal and transversal plasmon bands were 612 and 520nm, respectively. After being reduced by $NaBH_4$ from $Hg^{2+}$ to $Hg^0$, mercury and gold amalgamated, which led to the blue shift of the maximum absorption wavelength of longitudinal plasmon bands. As the concentration of $Hg^{2+}$ increased, the aspect ratio decreased. When concentration of mercury ions reached $1.57\times10^{-4}$M, there was only one absorption band present and spherical nanoparticles were formed. This method

proposed a practical way for the detection of $Hg^{2+}$ in tap water samples at the parts-per-trillion level. The detection limit was$3.3\times10^{-15}$ M and the correlation coefficient was 0.998 in the range of $9.98\times10^{-14}$ to $1.5\times10^{-10}$M, which was 3 orders of magnitudes better than conventional analytical methods based on expensive instrumentation and showed great potential for the detection of ultralow contents of $Hg^{2+}$ in water samples. The whole procedure was rather simple and fast, and it took less than 10 min per sample, which was quite appropriate in on-site monitoring of $Hg^{2+}$.

Huang et al. [57] also utilized Au NRs for the detection of $Hg^{2+}$ based on amalgamation of gold and mercury, which could amplify the localized surface plasmon resonance signals. At first, Au NRs were end-to-end assembled via electrostatic interactions by $Na_3PO_4$, which possessed collective properties from coupling of optical and electronic properties between neighboring individual nanorods. With the addition of $Hg^{2+}$, $Hg^{2+}$ was reduced to $Hg^0$ by $NaBH_4$, and deposited on the surface of Au NRs, resulting in the amalgamation of Hg and Au and the blue shift of the SPR band. The gradual blue shift of SPR band was observed with the increased concentration of $Hg^{2+}$. When the concentration of $Hg^{2+}$ achieved $10^{-5}$M, the longitudinal and transversal absorption bands were overlap, and only one SPR band occurred. The LOD of this method was $10^{-13}$M, which was much lower than the results obtained from traditional methods. For example, Jia et al.[14] described a method that combing ionic liquid based dispersive liquid-liquid microextraction (IL-DLLME) with high performance liquid chromatography-inductively coupled plasma mass spectrometry (HPLC-ICP-MS) to determine the content of mercury species in liquid cosmetic samples and the detection limit was 1.3 ng/L for $Hg^{2+}$. In recent years, the detection systems for $Hg^{2+}$ based on Au NPs have been superior to conventional approaches in many aspects, including simplicity, accuracy, practicability and so on.

Compared with Au NPs, gold nanoclusters (Au NCs) have higher fluorescence quantum yield and smaller size, which makes Au NCs exhibit discreet electronic states and size-dependent fluorescence.[61, 62]

Hu et al. [63] developed a rapid, highly selective and sensitive assay of $Hg^{2+}$ in

aqueous solutions based on the fluorescence quenching of BSA-modified gold nanoclusters (BSA-Au NCs).The as-prepared BSA-Au NCs could dispersed uniformly in solution and fluoresced at 652nm when excited at 334nm, with a quantum yield of 6%. The fluorescence intensity of BSA-Au NCs decreased as the concentration of $Hg^{2+}$ increased. This assay relied on the high complexation of BSA-Au NCs with$Hg^{2+}$ by Hg-S bond (via the 35 Cys residues in BSA) and hence, possessed excellent selectivity. The method had the LOD of 80nM and got the satisfactory recoveries (95%-106.5%) of mercury ions by using standard addition method in different water samples such as river water, tap water and mineral water.

Xie et al. [64] also demonstrated a simple label-free method for detection of $Hg^{2+}$ based on fluorescence quenching of BSA-AuNCs and the high-affinity of metallophilic $Hg^{2+}$and $Au^{+}$. This one-step method was simple, fast, highly selective, and ultrasensitive (LOD was 0.5 nM). The strategy might be further developed as a simple paper test strip system for the rapid monitoring of $Hg^{2+}$, which might be as convenient as pH test paper and be very useful tool in resource-poor settings. Wei et al. [65]demonstrated a way to detect$Hg^{2+}$ based on Lysozyme-stabilized gold nanoclusters (Lys-Au NCs). In this assay, the fluorescent gold nanoclusters had an average size of 1nm and two emission peak at 445nm and 657nm. The fluorescent quantum yield of 657 nm emission was about 5.6%. The detection range was tunable using varied concentration of Lys-Au NCs. When using 1% Lys-Au NCs, the detection range of $Hg^{2+}$ could be tuned from 10nM to 5000nM. The detection systems developed recently based on Au NCs have solved many problems traditional analytical methods brought along with their high accuracy and sensitivity in the detection of $Hg^{2+}$and meanwhile, have achieved comparable, even much higher accuracy, sensitivity and selectivity, which have put them in the first place for the rapid on-site monitoring of $Hg^{2+}$ in aqueous samples.

## 2.2 Carbon nanomaterials

### 2.2.1 Carbon nanotubes

Carbon nanotubes have been well developed for detection of trace elements in

solutions in terms of their conductivity and fluorescent properties. Carbon nanotubes combining with the DNA by π-π stacking between the nucleotide bases and the single-walled carbon nanotubes (SWCNTs)' sidewall were used to determine $Hg^{2+}$ on the basis of $Hg^{2+}$ interaction with the DNA, which caused the DNA depart from the carbon nanotubes and led to the change of the signal.[66-68]

Gao et al. [69]detected $Hg^{2+}$via ICD (induced circular dichroism) of ssDNA wrapped around SWCNTs for the first time(Figure 12).The coupling effects of the transition dipole moment between DNA and SWCNTs produced strong ICD signal. In the presence of $Hg^{2+}$, it bound with DNA, which weakened the interaction between the DNA and SWCNTs and led to a part of DNA detached from the SWCNT surface. The ICD spectra showed that the intensity of ICD signal decreased significantly and the results of AFM revealed that DNA pith increased along the SWCNTs when the concentration of $Hg^{2+}$ increased. This method had an LOD of the nM level.

Zhang et al. [70]utilized the carbon nanotube-DNA hybrid fluorescent sensor for the detection of $Hg^{2+}$. A T-rich ssDNA was used as a fluorescence probe. In the absence of $Hg^{2+}$, the ssDNA wrapped around SWNTs and the fluorescence of dye was quenched. Upon addition of $Hg^{2+}$, the ssDNA and $Hg^{2+}$ formed a double helical structure via T-$Hg^{2+}$-T base pairs, which detached from the nanotubes surface and led to an increase of fluorescence emission comparable to the fluorescence of the ssDNA/carbon nanotubes complexes. The LOD of this method was 14.5 nM with high selectivity against other metal ions like $Cd^{2+}$, $Pb^{2+}$, and $Ca^{2+}$ etc. The advantage this method possessed over other analytical methods was that the selectivity and specificity for the detection of $Hg^{2+}$ were achieved by the specific binding ability of $Hg^{2+}$ to thymine bases and the interaction between SWNTs and ssDNA. Guo et al. [71] proposed a turn-on fluorescence method for $Hg^{2+}$ by using assembly of ssDNA, dye and SWCNTs. The SWNCTs, ssDNA, organic dye (Sybr Green I) formed a self-assembly system which resulted in the quenching of the dye's fluorescence. When the $Hg^{2+}$ and another T-rich ssDNA were added, the Sybr Green I intercalated into the dsDNA formed by T-$Hg^{2+}$-T mismatch and was removed from the surface of SWCNTs, which disturbed the reaction between the dye and SWCNTs and led to the

fluorescence restoration. This approach did not need fluorophore labeled oligonucleotide, and provided high sensitivity (the LOD is 7.9 nM) and selectivity (40-fold with other metal ions). In order to verify the practicability of the proposed method, it was applied to determine $Hg^{2+}$ in tap water samples that had been spiked with $Hg^{2+}$ at three different concentration levels before the detection. The results were in keeping with the found and added values.

### 2.2.2 Carbon nanoparticles

Carbon nanoparticles possess biocompatible and chemically inert properties. They are small and water soluble, which make them promising candidates for biological labeling and metal ions detections. Li et al. [72] developed a novel fluorescent strategy based on carbon nanoparticles for the determination of $Hg^{2+}$. The carbon nanoparticles were collected from candle soot, with a fluorescence emission at 518nm when excited at 480nm.Carbon nanoparticles quenched the fluorescence of the dye labeled on ssDNA via π-π stacking interaction between ssDNA and carbon nanoparticles. In the presence of $Hg^{2+}$, ssDNA departed from carbon nanoparticles surface due to the induced hairpin structure. This strategy had an LOD of 10nM, and superior selectivity against other possible metal ions. The approach was employed to analyze the environmental water with spiked $Hg^{2+}$and satisfied results that could be comparable to that of ICP-MS was achieved.

Li et al. [73] further demonstrated the fluorescent detection of mercury ions via nano-$C_{60}$ and a FAM-labeled $Hg^{2+}$-specific oligonucleotide probe. Nano-$C_{60}$ had a negatively charge surface and was an excellent electron acceptor. $C_{60}$ bound strongly to ssDNA through the imperceptibly electrostatic interactions as well as the π-π stacking interactions. Hence, the fluorescently labeled ssDNA probe adsorbed on the nano-$C_{60}$ led to substantial fluorescence quenching. In the presence of $Hg^{2+}$, the conformation of oligonucleotide folded into hairpin structure via T-$Hg^{2+}$-T base pair, which did not adsorb on nano-$C_{60}$ and suppressed the quenching, thus signaled the existence of the target (Figure 13).This strategy achieved the detection limit as low as 500pM, which is lower than the toxicity level of $Hg^{2+}$ in drinking water (10 nM)

defined by U.S. EPA. The application of the proposed method in real sample analysis was investigated to verify its utilization. The water samples detected were obtained from the South Lake of Changchun, China. Results demonstrated that the detection was not affected by the disturbance of bacteria, pathogens and other materials in the lake, which made this approach possible for the detection of $Hg^{2+}$ in much more complicated samples in the environment.

### 2.3 Quantum dots

Quantum dots (QDs) have attracted much attention for its uniquely optical and electronic properties, such as excellent fluorescence quantum yields, photobleaching threshold and photostability. In recent years, QDs have been widely used for chemical sensing through the change of photoluminescence induced by analytes.[74, 75]

For the detection of $Hg^{2+}$ using QDs, the principle of T-$Hg^{2+}$-T coordination and Hg-S interaction could also be used. Besides, since QDs had high photoluminescence quantum yield, they were used as “turn on” or “turn off” fluorescent probes.[76-79]

Functionalized CdSe/ZnS QDs were attractive for detecting $Hg^{2+}$since $Hg^{2+}$ could quench the fluorescence of function group modified CdSe/ZnS QDs. In addition, the ligands modified on the CdSe/ZnS QDs played a core role on fluorescence response of specific metal ions. The water-soluble L-cysteine functionalized CdSeQDs with high stability and fluorescence quantum yield were used as fluorescence probe for $Hg^{2+}$.[80] Nanoparticles in this approach displayed some unique properties that distinguished them from traditional organic fluorophores, such as stability against photobleaching and blinking. The approach was based on the fact that $Hg^{2+}$had high affinity to the amide group, which led to the effective electron transfer process on the surface of QDs between the $Hg^{2+}$and the functional group. A good linear relationship between the fluorescence intensity ratio and the concentration of $Hg^{2+}$ was obtained and the detection limit was 6nM. Moreover, the method was testified by the application on the real sample of human urine and river water, and achieved satisfactory results with the recovery of $Hg^{2+}$ in the range of 95-101% that were in keeping with the results obtained from cold vapor atomic fluorescence

spectrometry (CV-AFS), which suggested that the method was practical and credible.

Freeman et al. [75]used CdSe/ZnS QDs to detect $Hg^{2+}$ and $Ag^{+}$ simultaneously by modifying two types of different and specific nucleic acids, which exhibited two emission bands of fluorescence spectra. $Hg^{2+}$ quenched the fluorescence of CdSe/ZnS QDs when it was modified with a thymine-rich nucleic acid, which was attributed to the electron transfer process caused by the bond of $Hg^{2+}$ with thymine. L-carnitine capped CdSe/ZnS QDs were applied for the detection of $Hg^{2+}$ in ethanol.[81] In this approach, $Hg^{2+}$acted as a quencher via electron transfer from L-carnitine to $Hg^{2+}$, and the detection limit of $Hg^{2+}$ concentration was 18μM. N-acetyl-L-cysteine capped ZnS quantum dots (NAC-ZnS QDs) synthesized via a one-step method in aqueous solutions by using inexpensive and safe materials were also used as fluorescent probes for quantitative determination of $Hg^{2+}$ (Figure 14).[82]In the presence of $Hg^{2+}$, the fluorescence of NAC-ZnS QDs was quenched and the intensity of florescence was inversely proportional to concentration of mercury ions, which resulted from the electron transfer between ZnS QDs and $Hg^{2+}$. This method proved high sensitivity (LOD was 5nM) and excellent selectivity. Satisfactory results were obtained for the detecting of $Hg^{2+}$ in the tap water and spring water and the recovery of mercuryions was in the range from 94.5%-101.3%, which were in good agreement with the results achieved from CV-AFS and suggested the reliability and practicability of this method in the detection of $Hg^{2+}$ in aqueous environment.The advantages of this method such as the simple synthesis procedure, high sensitivity, excellent selectivity, reliability and practicability made it different from conventional methods and more promising in the application for detecting $Hg^{2+}$.

### 2.4 Silver nanomaterials

Silver nanomaterials have been widely used as antibacterial, antistatic, and cryogenically superconducting materials, etc. Besides, they have also been used to detect mercury in recent years. For example, Roy et al. [83]used Vitamin B2 (riboflavin) stabilized silver nanoparticles (Ag NPs)to detect $Hg^{2+}$ for the fact that $Hg^{2+}$had high affinity to the amino nitrogen of the thymine moiety of riboflavin. As a result, $Hg^{2+}$

replaced the Ag NPs to form a covalent structure with riboflavin. Riboflavin was a fluorescent molecule, the color changed from bright yellow to deep orange and the fluorescence was quenched immediately in the formation procedure of the riboflavin stabilized Ag NPs (R-Ag NPs). In the presence of $Hg^{2+}$, the color changed back to yellow and the fluorescence resumed. Interferential metal ions did not show the same phenomenon. On the other hand, R-Ag NPs had two absorption bands under UV/vis spectra, and only $Hg^{2+}$ decreased the absorption intensity heavily. In this approach, the time of sensing was one minute and the LOD for $Hg^{2+}$was 5nM, which demonstrated its feasibility in the rapid on-site detection of $Hg^{2+}$ as per U.S. EPA toxicity level of $Hg^{2+}$ in drinking water. According to the method, the $Hg^{2+}$ in tannery waste water (8.20 nM) and tap water (3.27 nM) were successfully detected.[83] Conventional analytical methods such as ICP-MS and CV-AFS had many disadvantages like the complicated preparation of samples before testing, the heavy dependence on expensive instrumentation and labor force. Although they could achieve comparable accuracy and sensitivity, they are no longer suited in modern analysis and detection of $Hg^{2+}$ that require simplicity, higher sensitivity and selectivity.

Tharmaraj and Pichumani[84] used Rh6G as a spectroscopic probe for detecting mercury using alginate stabilized silver nanocubes (alginate-Ag NCbs). In this approach, the fluorescence intensity of Rh6G decreased when it was attached on the surface of alginate-Ag NCbs and the solution displayed yellow. With the addition of $Hg^{2+}$, $Hg^{2+}$ formed amalgam-like structure with alginate-Ag NCbs and released the Rh6G from the surface of alginate-Ag NCbs. The fluorescence of Rh6G was restored and increased from yellow to purple with the concentration of $Hg^{2+}$improved. The detection limit for $Hg^{2+}$was $5.0\times10^{-11}$ M under the fluorescence response, which was much lower than that of some conventional methods.

Guo et al. tried the label-free detection of $Hg^{2+}$ based on protein-directed silver clusters.[76] The denatured bovine serum albumin coated silver nanoclusters (dBSA-Ag NCs) were utilized as fluorescent probes for$Hg^{2+}$ sensing, which relied on the quenching of the fluorescence of as-prepared silver clusters on the basis of $5d^{10}(Hg^{2+})$-$4d^{10}(Ag^{+})$ metallophilic interaction. In this approach, the 1nm dBSA-Ag

NCs showed high fluorescence emission at 637nm and high stability in high ionic conditions. In the presence of $Hg^{2+}$, dBSA-Ag NCs changed the color from light yellow to brown, and its fluorescence was sensitive and proportionately decreased with the concentration of $Hg^{2+}$increased. PDCA was used as a masking ligand to minimize other ions. The LOD for $Hg^{2+}$ in this assay was 10nM with the linear range from 10nM to5μM,[76] which was comparable to that obtained from traditional methods and met the limitation of $Hg^{2+}$ detection requirement by U.S. EPA in drinking water and predicted the application prospects of this method in real samples from the environment.

Another type of silver nanomaterials used for the detection of $Hg^{2+}$ was silver quantum dots (Ag QDs). The 2.7nm Ag QDs exhibited a SPR band at 395nm. In the presence of $Hg^{2+}$, $Hg^{2+}$ absorbed on the surface of Ag QDs via electrostatic attraction and caused the small red shifted and intensity decrease of SPR band. The calibration plot of intensity of SPR absorption band against the concentration of $Hg^{2+}$ was obtained in the concentration range between 50-350pM. The present method was simple without other group modified on the surface of Ag QDs, highly sensitive with the detection limit at 50pM, and also got excellent selectivity in the tenfold of other metal ions. At the same time, the authors proposed the other approach that used Ag QDs dispersed in amine functionalized silicate SG (SG-Ag QDs) to improve the detection limit (LOD was 5pM) and selectivity (50 fold against other metal ions) based on the higher affinity between the mercury and amine groups.[85] Generally, the detection limits of conventional method are about nM level. This assay improved the sensitivity and simplicity of $Hg^{2+}$ detection methods by using the optical and electronic properties of Ag QDs, which made it significant in the study of $Hg^{2+}$ detection.

### 2.5Silica nanoparticles

The design of most nanomaterials utilized for $Hg^{2+}$ detection was based on the interaction of $Hg^{2+}$ with thymine. Silica nanoparticles (Si NPs) utilized on detection of $Hg^{2+}$ also took this mechanism. Wang et al.[79] presented a fluorescence “turn on”

assay for $Hg^{2+}$detection by utilizing cationic conjugated polymers (CCP) and Si NPs to amplify the fluorescence. In this assay, dsDNA containing three pairs of T mismatches was attached on the surface of Si NPs. In the presence of $Hg^{2+}$, T-$Hg^{2+}$-T coordination was formed to capture Fl-labeled DNA on the surface of Si NPs during thermal wash and the complexation increased the melting temperature of the resulting duplex. Other ions could not form stable metal-DNA complex and there was weak or no fluorescent signals on the surface of nanoparticles. At last, cationic conjugated polymers were added to amplify fluorescence signal of the DNA combined with the fluorescein that remained on the surface of Si NPs. The working curve of $Hg^{2+}$ showed a sigmoidal shape and the detection limit was 100 nM. When the ratio of $Hg^{2+}$ and DNA duplex was kept at 3:1, the detection limit could be as low as 5 nM, which was lower than the limit of $Hg^{2+}$concentration in drinking water (10 nM) defined by U.S. EPA and could be used in the detection of real samples. With the assistance of CCP, the $Hg^{2+}$ detection assay showed great potential in environmental applications and industrial process control.

Zhu et al. [86]studied a highly sensitive and selective electrochemiluminescent (ECL) method for determination of $Hg^{2+}$ by using tris(2,2'-bipyridine)ruthenium(II) [$Ru(bpy)_3^{2+}$]-doped silica nanoparticles (Ru-Si NPs). At first, two mismatched ssDNA were modified on the electrode, one of which was labeled with Ru-Si NPs that was attached to oligonucleotides containing more $Ru(bpy)_3^{2+}$ and showed much stronger intensity of ECL than that of $Ru(bpy)_3^{2+}$ directly labeled to oligonucleotides. In the absence of $Hg^{2+}$, intensity of ECL for two ssDNA was low. With the addition of $Hg^{2+}$, two mismatched ssDNA switched to completely matched dsDNA, which eliminated the block of the electron transfer and increased the intensity of ECL. The detection limit for $Hg^{2+}$ was 2.3 nM and competing ions could coexist with $Hg^{2+}$ even if their concentrations were 50 times higher than that of $Hg^{2+}$. This method has been applied to detect $Hg^{2+}$ concentration in waste water samples and the results indicated that the average concentration of $Hg^{2+}$ in samples was 7.8 nM, which was in good agreement with the results obtained from AAS (8.0 nM).

## 3. Speciation of Mercury

The toxicity of mercury varies with its chemical forms. Different forms of mercury possess different bioavailability and toxicity. Elemental mercury ($Hg^0$), mercuric ions ($Hg^{2+}$), and organic mercury complexes such as methylmercury ($CH_3Hg^+$) are the three major mercury species. Microbial activities can lead to the methylation of water-soluble$Hg^{2+}$to $CH_3Hg^+$, the most toxic forms of Hg, which can accumulate and magnify through food chains.[87, 88]It is desired to study not only the inorganic mercury species like $Hg^{2+}$ but also the organic mercury species like $CH_3Hg^+$ since the latter is the most toxic form of Hg. In general, different Hg species can be quantified through the combination of chromatographic separation (gas chromatography or high performance liquid chromatography) hyphenated with element-specific spectrometry or molecular mass spectrometry,[89-91] including HPLC-ICP-MS,[92] HPLC-HG-AFS[93] and CE-ICP-MS[94], etc. These approaches provide excellent separate efficiency and low detection limits, but with high cost[95].

Nanomaterials are not only promising in the detection of $Hg^{2+}$ as mentioned above, but also have been used for the speciation of different mercury species. Chang et al. [96] proposed a "turn on" fluorescent probe based on bovine serum albumin, 3-mercaptopropionic acid and Rhodanmine 6Gmodified gold nanoparticles (BSA@R6G/MPA-Au NPs) to achieve the speciation of mercury species in aqueous solutions. This probe was operated under the mechanism that mercury ions bound with the Au NPs to release R6G from the Au NPs surface and recovered its fluorescence. In the presence of masking agent (EDTA and $Na_2S$), this probe could be used for specific detecting of $PhHg^+$ and the LOD was 20nM. Besides, while using tellurium nanowires (Te NWs) as making agent, the LOD of $PhHg^+$ could be as low as 10nM. River, sea and tap water and fish samples were analyzed to validate the feasibility of this rapid detection method of mercury species in the environmental and biological samples. Each sample was filtered and diluted prior to analysis. With the masking agent, the recoveries of $PhHg^+$ in the river, sea and tap water were 92.8%,

95.7% and 96.9%, while the recoveries of total organic mercury species were 90.5%, 100.5% and 109.6%, respectively. The results showed that by using this method such high recoveries became realizable from complicated, highly saline seawater samples and indicated the feasibility of the BSA@R6G/MPA-Au NP system in the detection of mercury in environmental samples. Moreover, the concentration of $CH_3Hg^+$ in the certified reference material dogfish muscle (DORM-2) was analysis by this approach, and the results were in good accordance with the results achieved by ICP-MS. Thereby, this strategy held great potential for mercury species analysis of environmental and biological samples.

Lin et al. [97] presented a "turn off" fluorescence sensor based on Lysozyme Type VI-stabilized gold nanoclusters (Lys VI-Au NCs) for detecting mercuric ions and methylmercury ions in seawater. The mechanism of this approach was through the interaction between $Hg^{2+}$ or $CH_3Hg^+$ and $Au^+$ on the surface of Lys VI-Au NCs. The quantum yield of Lys VI-Au NCs was approximately 9% and the amount of $Au^+$ on the Lys VI-Au NCs was calculated to be 41%. The fluorescent intensity of Lys VI-Au NCs decreased significantly at 631nm after the addition of $Hg^{2+}$ or $CH_3Hg^+$. The correlation coefficient was 0.9949 among the concentration range of 10-1200nM and the LOD was 3pM for $Hg^{2+}$, while the correlation coefficients was 0.9904 and LOD was 4nM for $CH_3Hg^+$ among the concentration range of 15-2000nM. The fluorescence of Lys VI-Au NCs decreased with the concentration of spiked $Hg^{2+}$ or $CH_3Hg^+$ in seawater increased. The LOD for $Hg^{2+}$and $CH_3Hg^+$ was 0.51nM and 5.90nM, respectively. While comparing to conventional methods and other Au NC-based sensors, this method displayed good selectivity and lower detection limit in the determination of $Hg^{2+}$. Besides, the application of this method in complex environment has also been validated.

The above mentioned studies stated less about the detection of both $Hg^{2+}$and$CH_3Hg^+$. Chen et al. [98] studied the determination of $CH_3Hg^+$ co-existing with $Hg^{2+}$ based on the fluorescence quenching of bovine serum albumin stabilized gold nanoclusters (BSA-Au NCs). It was found that the fluorescence quenching of BSA-Au NCs by $Hg^{2+}$was stronger than that caused by the same concentration of

$CH_3Hg^+$. $Hg^{2+}$could be masked by EDTA while $CH_3Hg^+$was less affected. Therefore, the determination of $CH_3Hg^+$ was achieved through EDTA masking. The detection limit for $CH_3Hg^+$was 35 nM after masking $Hg^{2+}$ with EDTA. This method has been successfully applied to quantify $CH_3Hg^+$ in rice paddy water from Qingzhen, Guizhou and tap water from Beijing.

## 4. Conclusions

Facing the challenges of sensitive, rapid, and cost-effective detection of mercury, nanomaterials have attracted much attention for their uniquely optical and physicochemical characters. Most of nanomaterials-based approaches for the detection of $Hg^{2+}$relied on the $Hg^{2+}$ interactions with T-T mismatch to form T-$Hg^{2+}$-T coordination. Despite the high affinity of DNA with $Hg^{2+}$, these approaches had some drawbacks, one of which was the difficulty researchers encountered while synthesizing the probes. Colorimetric sensors for $Hg^{2+}$detection based on the direct interaction between Hg and Au/Ag generated direct observations that could easily be visible by naked eyes and were suitable for on-site determination. However, the sensitivity of these sensors and their applications in real samples from complex systems are still problems. Hence, it is urgent to improve colorimetric sensors' sensitivity and increase their applications in real samples. Taking the complexity of real samples into consideration, the complicated matrix effect of real samples should be put first to avoid potential problems that may prevent the applications of these sensors in complex systems while designing colorimetric sensors. In terms of the "turn on" or "turn off" fluorescent probes based on nanomaterials, they played promising roles for the detection of $Hg^{2+}$, but a part of these assays were time-consuming on the preparation of the fluorescent probes and needed the addition of masking agents to improve the selectivity. Most of these methods had the LOD below 10 nM, which was lower than the limit of $Hg^{2+}$ in drinking water defined by U.S. EPA.

Nanomaterials have also been used for the speciation of mercury and are promising in the application to environmental and biological samples, although it has

not been so extensively studied as that on the detection of $Hg^{2+}$. Masking agents are generally necessary for the speciation of different mercury species. Hence, there are much more efforts needed to develop some kinds of approaches that are highly sensitive, selective, simple, and suitable for on-site and real samples based on nanomaterials. In addition, to avoid the potential of secondary pollution, the toxicology and bio-effects of nanomaterials are also needed to be studied prior to the wider application.[25, 26]

## Acknowledgement

This work was financially supported by National Natural Science Foundation of China (11205168, 11375213, 11475196 and U1432241). Y-F Li gratefully acknowledges the support of K. C. Wong Education Foundation, Hong Kong and the CAS Youth Innovation Promotion Association, Chinese Academy of Sciences (2011017).C Chen acknowledges the National Science Fund for Distinguished Young Scholars (11425520).

## References

1. L. Amin-Zaki, S. Elhassani, M. A. Majeed, T. W. Clarkson, R. A. Doherty and M. Greenwood, *Pediatrics*, 1974, **54**, 587-595.
2. N. Mori, A. Yasutake and K. Hirayama, *Arch. Toxicol.*, 2007, **81**, 769-776.
3. N. Mori, A. Yasutake, M. Marumoto and K. Hirayama, *J. Toxicol. Sci.*, 2011, **36**, 253-259.
4. P. Selid, H. Xu, E. M. Collins, M. Striped Face-Collins and J. X. Zhao, *Sensors*, 2009, **9**, 5446.
5. A. Yasutake and M. Nakamura, *J. Toxicol. Sci.*, 2011, **36**, 365-372.
6. W. Zheng, M. Aschner and J.-F. Ghersi-Egea, *Toxicol. Appl. Pharmacol.*, 2003, **192**, 1-11.
7. Z. Zhu, G. C. Y. Chan, S. J. Ray, X. Zhang and G. M. Hieftje, *Anal. Chem.*, 2008, **80**, 7043-7050.
8. Z. Zhu, Z. Liu, H. Zheng and S. Hu, *J. Anal. At. Spectrom.*, 2010, **25**, 697-703.
9. P. R. Aranda, R. A. Gil, S. Moyano, I. De Vito and L. D. Martinez, *J. Hazard. Mater.*, 2009, **161**, 1399-1403.
10. D. Han, Y.-R. Kim, J.-W. Oh, T. H. Kim, R. K. Mahajan, J. S. Kim and H. Kim, *Analyst*, 2009, **134**, 1857-1862.
11. Y. He, S. Zhang, X. Zhang, M. Baloda, A. S. Gurung, H. Xu, X. Zhang and G. Liu, *Biosens. Bioelectron.*, 2011, **26**, 2018-2024.
12. F. Pena-Pereira, I. Lavilla, C. Bendicho, L. Vidal and A. Canals, *Talanta*, 2009, **78**, 537-541.

13. X. Wu, W. Yang, M. Liu, X. Hou and C. Zheng, *J. Anal. At. Spectrom.*, 2011, **26**, 1204-1209.
14. X. Jia, Y. Han, C. Wei, T. Duan and H. Chen, *J. Anal. At. Spectrom.*, 2011, **26**, 1380-1386.
15. Y.-F. Li, C. Chen, B. Li, J. Sun, J. Wang, Y. Gao, Y. Zhao and Z. Chai, *J. Anal. At. Spectrom.*, 2006, **21**, 94-96.
16. S. Ando and K. Koide, *Journal of the American Chemical Society*, 2011, **133**, 2556-2566.
17. M. H. Lee, J.-S. Wu, J. W. Lee, J. H. Jung and J. S. Kim, *Org. Lett.*, 2007, **9**, 2501-2504.
18. Y. Yang, Y. Wang and Y. Peng, *Sci. China Chem.*, 2014, **57**, 289-295.
19. Y. Zhang, B. Shi, P. Zhang, J. Huo, P. Chen, Q. Lin, J. Liu and T. Wei, *Sci. China Chem.*, 2013, **56**, 612-618.
20. I.-B. Kim and U. H. F. Bunz, *J. Am. Chem. Soc.*, 2006, **128**, 2818-2819.
21. X. Liu, Y. Tang, L. Wang, J. Zhang, S. Song, C. Fan and S. Wang, *Adv. Mater.*, 2007, **19**, 1471-1474.
22. X. Ren and Q.-H. Xu, *Langmuir*, 2009, **25**, 29-31.
23. M. Hollenstein, C. Hipolito, C. Lam, D. Dietrich and D. M. Perrin, *Angew. Chem.*, 2008, **47**, 4346-4350.
24. F. Lao, L. Chen, W. Li, C. Ge, Y. Qu, Q. Sun, Y. Zhao, D. Han and C. Chen, *ACS Nano*, 2009, **3**, 3358-3368.
25. Y. Zhao and H. Nalwa, *Nanotoxicology: Interactions of Nanomaterials with Biological Systems*, American Scientific Publishers, 2007.
26. Y.-F. Li, J. Zhao, Y. Qu, Y. Gao, Z. Guo, Z. Liu, Y. Zhao and C. Chen, *Nanomedicine*, 2015, **11**, 1531-1549.
27. Y.-W. Lin, C.-C. Huang and H.-T. Chang, *Analyst*, 2011, **136**, 863-871.
28. J. J. McNerney, P. R. Buseck and R. C. Hanson, *Science*, 1972, **178**, 611-612.
29. J. Du, B. Zhu, X. Peng and X. Chen, *Small*, 2014, **10**, 3461-3479.
30. Y.-R. Kim, H. J. Kim, J. S. Kim and H. Kim, *Adv. Mater.*, 2008, **20**, 4428-4432.
31. D. Liu, W. Qu, W. Chen, W. Zhang, Z. Wang and X. Jiang, *Anal. Chem.*, 2010, **82**, 9606-9610.
32. X. Xu, J. Wang, K. Jiao and X. Yang, *Biosens. Bioelectron.*, 2009, **24**, 3153-3158.
33. J. Du, L. Jiang, Q. Shao, X. Liu, R. S. Marks, J. Ma and X. Chen, *Small*, 2013, **9**, 1467-1481.
34. P. K. Sudeep, B. I. Ipe, K. G. Thomas, M. V. George, S. Barazzouk, S. Hotchandani and P. V. Kamat, *Nano Lett.*, 2002, **2**, 29-35.
35. Y.-K. Yang, K.-J. Yook and J. Tae, *J. Am. Chem. Soc.*, 2005, **127**, 16760-16761.
36. S. Yoon, A. E. Albers, A. P. Wong and C. J. Chang, *J. Am. Chem. Soc.*, 2005, **127**, 16030-16031.
37. X. Xue, F. Wang and X. Liu, *J. Am. Chem. Soc.*, 2008, **130**, 3244-3245.
38. Y. Miyake, H. Togashi, M. Tashiro, H. Yamaguchi, S. Oda, M. Kudo, Y. Tanaka, Y. Kondo, R. Sawa, T. Fujimoto, T. Machinami and A. Ono, *J. Am. Chem. Soc.*, 2006, **128**, 2172-2173.
39. L. Wang, Y. Liu, W. Li, X. Jiang, Y. Ji, X. Wu, L. Xu, Y. Qiu, K. Zhao, T. Wei, Y. Li, Y. Zhao and C. Chen, *Nano Letters*, 2011, **11**, 772-780.
40. D. Li, A. Wieckowska and I. Willner, *Angew. Chem.*, 2008, **120**, 3991-3995.
41. C.-W. Liu, Y.-T. Hsieh, C.-C. Huang, Z.-H. Lin and H.-T. Chang, *Chem. Comm.*, 2008, DOI: 10.1039/B719856F, 2242-2244.
42. C.-W. Liu, C.-C. Huang and H.-T. Chang, *Langmuir*, 2008, **24**, 8346-8350.
43. J. Wu, L. Li, D. Zhu, P. He, Y. Fang and G. Cheng, *Anal. Chim. Acta*, 2011, **694**, 115-119.
44. N. Kanayama, T. Takarada and M. Maeda, *Chem. Comm.*, 2011, **47**, 2077-2079.

45. J.-S. Lee, M. S. Han and C. A. Mirkin, *Angew. Chem.*, 2007, **46**, 4093-4096.
46. J. Du, Y. Sun, L. Jiang, X. Cao, D. Qi, S. Yin, J. Ma, F. Y. C. Boey and X. Chen, *Small*, 2011, **7**, 1407-1411.
47. A. Zheng, J. Chen, G. Wu, H. Wei, C. He, X. Kai, G. Wu and Y. Chen, *Microchim. Acta*, 2009, **164**, 17-27.
48. J. Chen, A. Zheng, A. Chen, Y. Gao, C. He, X. Kai, G. Wu and Y. Chen, *Anal. Chim. Acta*, 2007, **599**, 134-142.
49. C.-C. Huang, Z. Yang, K.-H. Lee and H.-T. Chang, *Angew. Chem.*, 2007, **119**, 6948-6952.
50. D. J, S. Yin, L. Jiang, B. Ma and X. Chen, *Chem. Commun.*, 2013, **49**, 4196-4198.
51. J. Du, B. Zhu and X. Chen, *Small*, 2013, **9**, 4104-4111.
52. J. Du, B. Zhu, W.R. Leow, S. Chen, T.C. Sum, X. Peng and X. Chen, *Small*, 2015, **11**, 4104-4110.
53. H.-C. Huang, S. Barua, D. B. Kay and K. Rege, *ACS Nano*, 2009, **3**, 2941-2952.
54. H. Wang, T. B. Huff, D. A. Zweifel, W. He, P. S. Low, A. Wei and J.-X. Cheng, *Proc. Natl Acad. Sci. USA*, 2005, **102**, 15752-15756.
55. L. Wang, Y. Liu, W. Li, X. Jiang, Y. Ji, X. Wu, L. Xu, Y. Qiu, K. Zhao, T. Wei, Y. Li, Y. Zhao and C. Chen, *Nano Lett.*, 2011, **11**, 772-780.
56. C. V. Durgadas, V. N. Lakshmi, C. P. Sharma and K. Sreenivasan, *Sens. Actuat. B Chem.*, 2011, **156**, 791-797.
57. H. Huang, X. Liu, T. Hu and P. K. Chu, *Biosens. Bioelectron.*, 2010, **25**, 2078-2083.
58. G. J. Nusz, S. M. Marinakos, A. C. Curry, A. Dahlin, F. Höök, A. Wax and A. Chilkoti, *Anal. Chem.*, 2008, **80**, 984-989.
59. P. Jain, X. Huang, I. El-Sayed and M. El-Sayed, *Plasmonics*, 2007, **2**, 107-118.
60. M. Rex, F. E. Hernandez and A. D. Campiglia, *Anal. Chem.*, 2006, **78**, 445-451.
61. Y. Bao, C. Zhong, D. M. Vu, J. P. Temirov, R. B. Dyer and J. S. Martinez, *J. Phys. Chem. C*, 2007, **111**, 12194-12198.
62. J. Xie, Y. Zheng and J. Y. Ying, *J. Am. Chem. Soc.*, 2009, **131**, 888-889.
63. D. Hu, Z. Sheng, P. Gong, P. Zhang and L. Cai, *Analyst*, 2010, **135**, 1411-1416.
64. J. Xie, Y. Zheng and J. Y. Ying, *Chem. Commun.*, 2010, **46**, 961-963.
65. H. Wei, Z. Wang, L. Yang, S. Tian, C. Hou and Y. Lu, *Analyst*, 2010, **135**, 1406-1410.
66. S. N. Kim, J. F. Rusling and F. Papadimitrakopoulos, *Adv. Mater.*, 2007, **19**, 3214-3228.
67. Y. Liu, Y. Wang, J. Jin, H. Wang, R. Yang and W. Tan, *Chem. Comm.*, 2009, DOI: 10.1039/B819526A, 665-667.
68. R. Yang, J. Jin, Y. Chen, N. Shao, H. Kang, Z. Xiao, Z. Tang, Y. Wu, Z. Zhu and W. Tan, *J. Am. Chem. Soc.*, 2008, **130**, 8351-8358.
69. X. Gao, G. Xing, Y. Yang, X. Shi, R. Liu, W. Chu, L. Jing, F. Zhao, C. Ye, H. Yuan, X. Fang, C. Wang and Y. Zhao, *J. Am. Chem. Soc.*, 2008, **130**, 9190-9191.
70. L. Zhang, T. Li, B. Li, J. Li and E. Wang, *Chem. Comm.*, 2010, **46**, 1476-1478.
71. L.-q. Guo, N. Yin, D.-d. Nie, J.-r. Gan, M.-j. Li, F.-f. Fu and G.-n. Chen, *Analyst*, 2011, **136**, 1632-1636.
72. H. Li, J. Zhai, J. Tian, Y. Luo and X. Sun, *Biosens. Bioelectron.*, 2011, **26**, 4656-4660.
73. H. Li, J. Zhai and X. Sun, *Nanoscale*, 2011, **3**, 2155-2157.
74. M. Frasco and N. Chaniotakis, *Sensors*, 2009, **9**, 7266.
75. R. Freeman, T. Finder and I. Willner, *Angew. Chem.*, 2009, **48**, 7818-7821.

76. C. Guo and J. Irudayaraj, *Anal. Chem.*, 2011, **83**, 2883-2889.
77. L. E. Page, X. Zhang, A. M. Jawaid and P. T. Snee, *Chem. Comm.*, 2011, **47**, 7773-7775.
78. Z. B. Shang, Y. Wang and W. J. Jin, *Talanta*, 2009, **78**, 364-369.
79. Y. Wang and B. Liu, *Macromol. Rapid Comm.*, 2009, **30**, 498-503.
80. J. Chen, Y. Gao, Z. Xu, G. Wu, Y. Chen and C. Zhu, *Anal. Chim. Acta*, 2006, **577**, 77-84.
81. H. Li, Y. Zhang, X. Wang, D. Xiong and Y. Bai, *Mater. Lett.*, 2007, **61**, 1474-1477.
82. J. Duan, X. Jiang, S. Ni, M. Yang and J. Zhan, *Talanta*, 2011, **85**, 1738-1743.
83. B. Roy, P. Bairi and A. K. Nandi, *Analyst*, 2011, **136**, 3605-3607.
84. V. Tharmaraj and K. Pitchumani, *Nanoscale*, 2011, **3**, 1166-1170.
85. G. Maduraiveeran, V. Tamilmani and R. Ramaraj, *Curr. Sci.*, 2011, **100**, 199-204.
86. X. Zhu, L. Chen, Z. Lin, B. Qiu and G. Chen, *Chem. Comm.*, 2010, **46**, 3149-3151.
87. G. Deng, T. Zhang, L. Yang and Q. Wang, *Chin. Sci. Bull.*, 2013, **58**, 256-265.
88. F. Wang and J. Zhang, *Chin. Sci. Bull.*, 2013, **58**, 141-149.
89. Y.-F. Li, C. Chen, B. Li, Q. Wang, J. Wang, Y. Gao, Y. Zhao and Z. Chai, *J. Anal. At. Spectrom.*, 2007, **22**, 925-930.
90. M. Wang, W. Feng, J. Shi, F. Zhang, B. Wang, M. Zhu, B. Li, Y. Zhao and Z. Chai, *Talanta*, 2007, **71**, 2034-2039.
91. Y. Yin, J. Liu and G. Jiang, *Chin. Sci. Bull.*, 2013, **58**, 150-161.
92. I. Cattani, S. Spalla, G. M. Beone, A. A. M. Del Re, R. Boccelli and M. Trevisan, *Talanta*, 2008, **74**, 1520-1526.
93. J. L. Gómez-Ariza, D. Sánchez-Rodas, I. Giráldez and E. Morales, *Talanta*, 2000, **51**, 257-268.
94. T.-H. Lee and S.-J. Jiang, *Anal. Chim. Acta*, 2000, **413**, 197-205.
95. M. Leermakers, W. Baeyens, P. Quevauviller and M. Horvat, *Trends Anal. Chem.*, 2005, **24**, 383-393.
96. H.-Y. Chang, T.-M. Hsiung, Y.-F. Huang and C.-C. Huang, *Environ. Sci. Technol.*, 2011, **45**, 1534-1539.
97. Y.-H. Lin and W.-L. Tseng, *Anal. Chem.*, 2010, **82**, 9194-9200.
98. X. Chen, J. Zhao, W. Cong, X. Li, H. Fan, J. Sun, J. Lin, B. Li, Y. Gao, C. Qin and Y.-F. Li, *J. Nanosci. Nanotechnol.*, 2015, doi:10.1166/jnn.2015.10642.

**Figure captions**

Figure 1 Colorimetric detection of $Hg^{2+}$ using DNA-Au NPs. Reprinted with permission ref[17]. Copyright 2007Wiley.

Figure 2 Colorimetric detection of $Hg^{2+}$ based on DNA-Au NPs. Reprinted with permission ref[37]. Copyright 2008 ACS.

Figure 3 $Hg^{2+}$ induced colorimetric response of MTA-Au NPs, and color change of the solution in the presence of various representative metallic ions at concentrations of 100 μM. Reprinted with permission from ref [31]. Copyright 2010, ACS.

Figure 4 Colorimetric detection of $Hg^{2+}$ based on simply mixing Au NPs and oligopeptides. Reprinted with permission from ref [46]. Copyright 2011, Wiley.

Figure 5 Illustrations of Hg-induced ICD signal intensity change of DNA-SWCNTs. Reprinted with permission from ref[69]. Copyright 2008, ACS.

Figure 6 A schematic (not to scale) illustrating the nano-$C_{60}$-based fluorescent $Hg^{2+}$ detection based on the conformational change of a $Hg^{2+}$-specific T-rich OND ($P_H$). $P_H$: a FAM-labeled $Hg^{2+}$-specific OND probe. Reprinted with permission from ref[73]. Copyright 2011, RSC.

Figure 7 Schematic illustration for the fluorescence quenching of NAC-capped ZnS QDs by $Hg^{2+}$. Reprinted with permission from ref[82]. Copyright 2008, Elsevier.

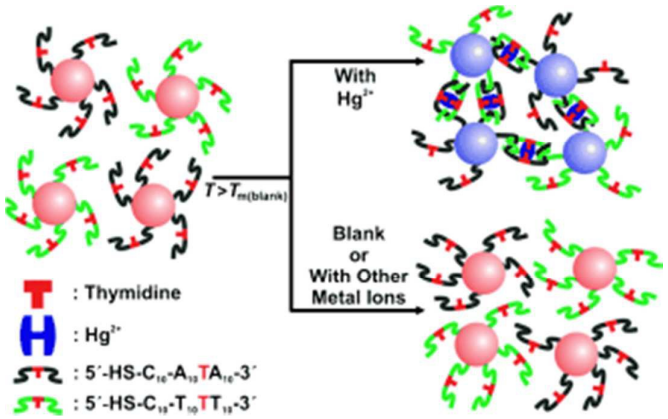


Figure 8 Colorimetric detection of $Hg^{2+}$ using DNA-Au NPs. Reprinted with permission ref[45]. Copyright 2007Wiley.

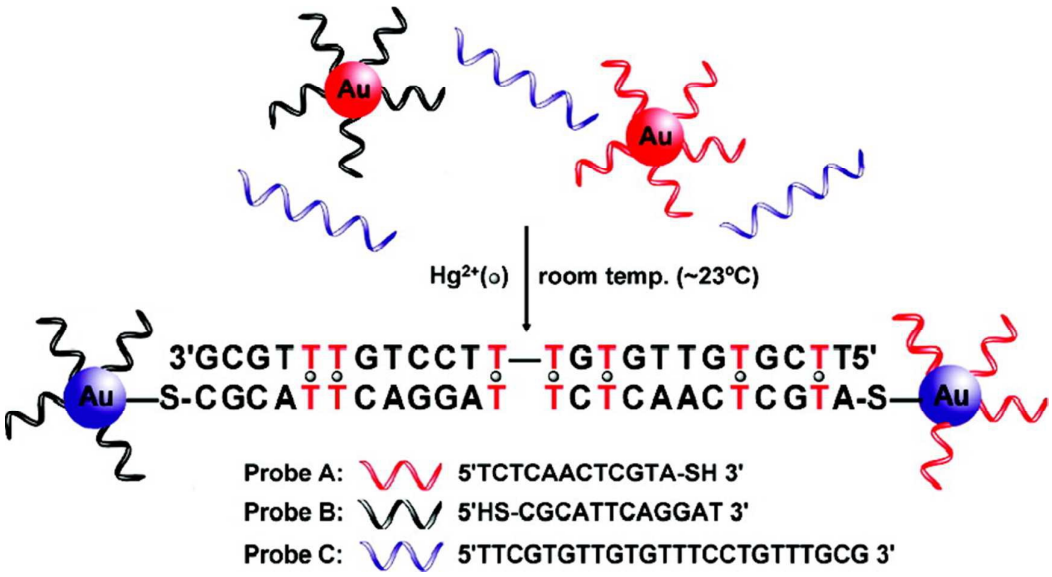


Figure 9 Colorimetric detection of $Hg^{2+}$ based on DNA-Au NPs. Reprinted with permission ref[37]. Copyright 2008 ACS.

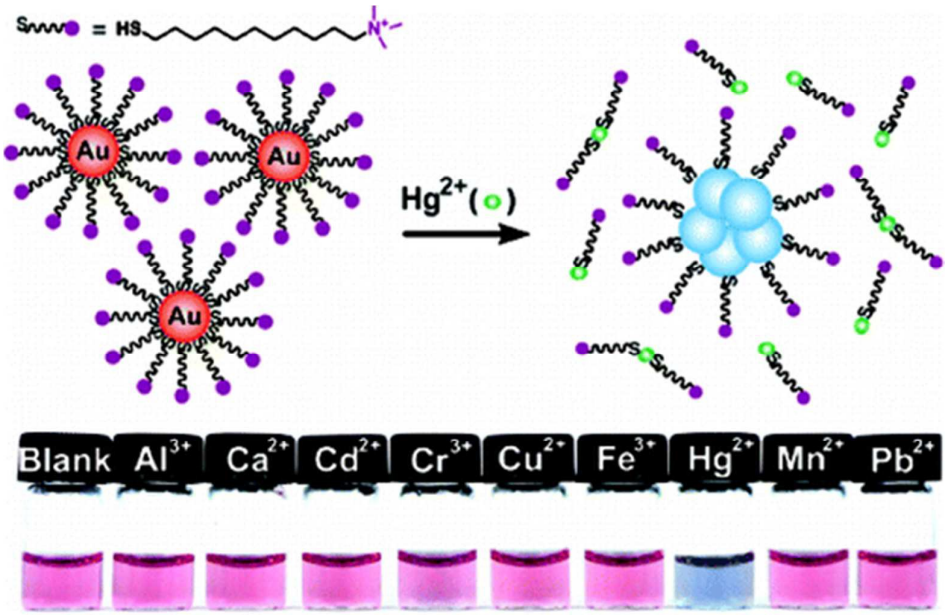


Figure 10 $Hg^{2+}$ induced colorimetric response of MTA-Au NPs, and color change of the solution in the presence of various representative metallic ions at concentrations of 100 μM. Reprinted with permission from ref [31]. Copyright 2010, ACS.

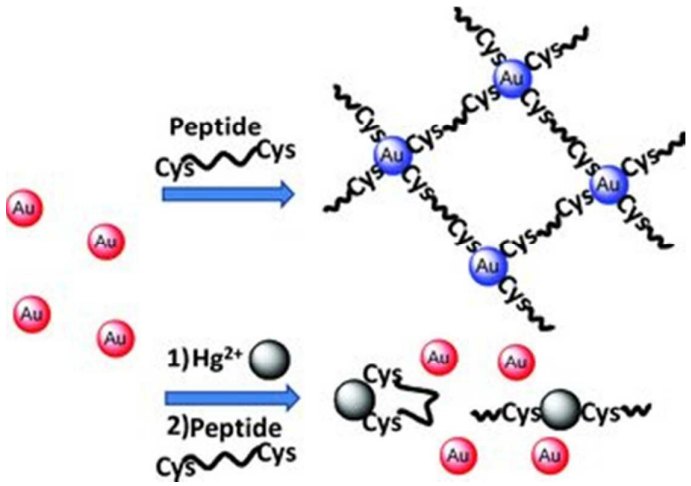


Figure 11Colorimetric detection of $Hg^{2+}$ based on simply mixing Au NPs and oligopeptides. Reprinted with permission from ref [46]. Copyright 2011, Wiley.

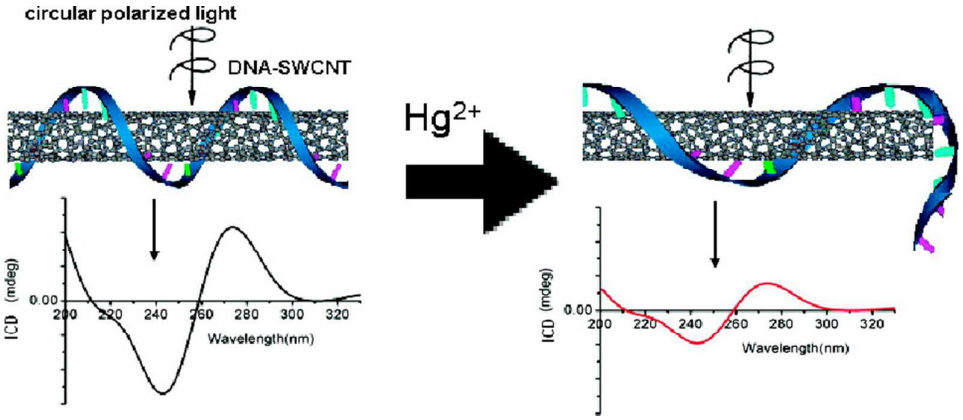


Figure 12 Illustrations of Hg-induced ICD signal intensity change of DNA-SWCNTs. Reprinted with permission from ref[69]. Copyright 2008, ACS.

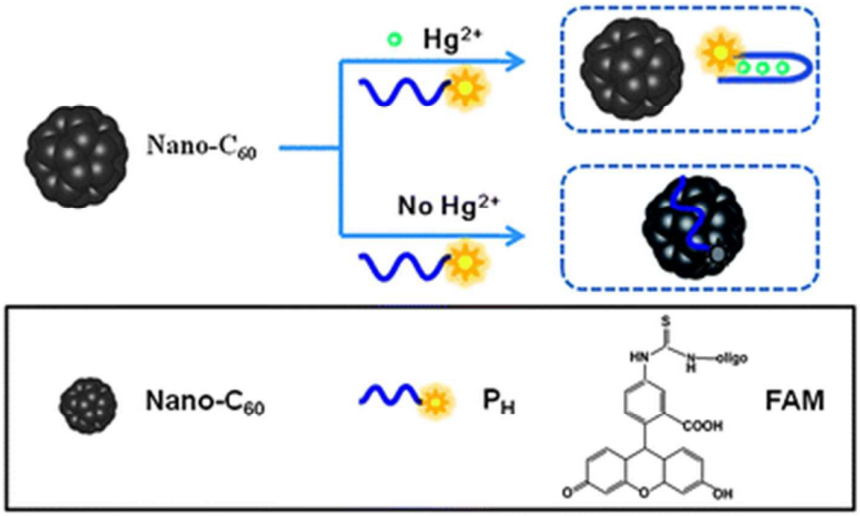


Figure 13 A schematic (not to scale) illustrating the nano-$C_{60}$-based fluorescent $Hg^{2+}$ detection based on the conformational change of a $Hg^{2+}$-specific T-rich OND ($P_H$). $P_H$: a FAM-labeled $Hg^{2+}$-specific OND probe. Reprinted with permission from ref[73]. Copyright 2011, RSC.

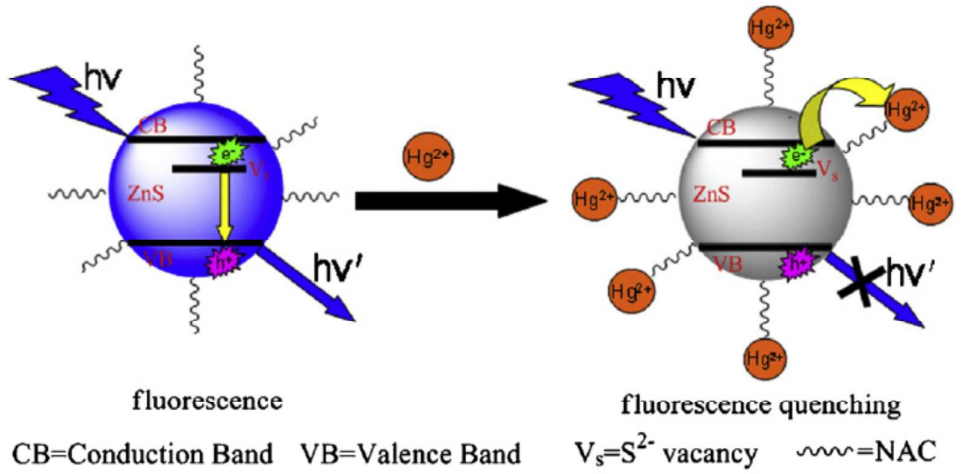


Figure 14 Schematic illustration for the fluorescence quenching of NAC-capped ZnS QDs by $Hg^{2+}$. Reprinted with permission from ref[82]. Copyright 2008, Elsevier.